Transactions of the Materials Research Society of Japan 24 [1] 125-128 (1999)

Adhesion and Fretting Behaviors of TiN, CrN and TiN/CrN Superlattices

Y.M.ZHOU, R.ASAKI, W.-H. SOE, R. YAMAMOTO

Institute of Industrial Science, University of Tokyo,7-22-1 Roppongi, Minato-ku, Tokyo, 106-8558 Japan

Fax: 81-3-3402-2629, e-mail: ymzhou@cc.iis.u-tokyo.ac.jp

R. CHEN, A. IWABUCHI

Iwate University, Ueda 4-3-5, Morika, 020-8551 Japan

Fax: 81-19-624-3951, e-mail: chenrong@iwate-u.ac.jp

Fretting wear experiments were conducted by means of ball-on-disc method to investigate the wear properties and mechanism of TiN, CrN and TiN/CrN superlattices deposited on WC/Co cemented substrate by reactive magnetron sputtering. For TiN/CrN superlattices, the enhancements of hardness, elastic modulus and the resistance to plastic deformation would contribute to the improvement of adhesion, the lowering of crack penetration rate, the decrease of friction coefficient and net wear volume. The friction coefficient of TiN/CrN superlattice films indicated a similar tendency with CrN single film that these values will decrease after 10^3 cycles and located from 0.15 to 0.25, however, CrN and TiN is 0.12 and 0.30 respectively. The net wear volume of TiN/CrN superlattices was one fifth of that of TiN after 5×10^4 cycle numbers. Almost no stuck particles from bearing ball wear observed on the surface of superlattices by scanning electron microscopy (SEM), SEM imaging and surface roughness profilometer. Adhesion behavior was improved by TiN/CrN superlattices technology as compared to TiN, CrN single films. The wear mechanism of TiN/CrN superlattices transferred from mixed stick-slip to gross slip regime.

Key words: TiN/CrN ceramic superlattices, Fretting Wear, Friction Coefficient, Adhesion,

1. INTRODUCTION

The tribological behaviors of single layer film TiN have been well researched and put into industrial application in tool, mould, bearing ball coatings etc. [1,2]. Researches have also been done for CrN coating deposited on HSS substrate for cutting non-ferrous materials and for precision mould surface protection recently [3-7], but it is difficult to impose CrN film to machine ferrous materials because of the high affinity with iron and low hardness value in comparison with TiN. However, the lower friction coefficient of CrN than TiN under the same wear condition, is an attractive issue for machining industry.

Ceramic superlattices, the so-called fourth generation of hard coatings (e.g. TiN/NbN, TiN/ZrN, TiN/TaN, TiN/CrN) [8-10], exhibit the anomaly of hardness due to Keohler effect and Hall-Petch effect [11-13]. These superlattices have been expected to possess superior mechanical and tribological properties like multilayer coatings [14], and to improve wear resistance, toughness, fatigue life etc.

Zhang Renji et al [15] developed the wear mechanism of multilayers, as for CVD TiC-TiN multilayer coating. The cracks in the multilayer coating cannot always propagate in a given direction because there are no columnar crystal in the multilayer coating, the existing of interfaces and the grains in it are finer than in single layer films. Then the crack propagation rate is also lower than that in a single layer film. The sliding wear behaviors and fretting wear characteristics of Ni/Cu metal – metal superlattices were carried out [16] and the mechanism of fretting wear for metal – metal multilayer films were adhesion and fatigue.

Although fretting is the small amplitude oscillatory movement which occur between the contacting surfaces [17], it has been known as an effective assessment method to understand some physical, chemical and mechanical phenomena (friction coefficient, wear volume, adhesive, debris, interaction, oxidation, fatigue, crack etc) directly from the fretting results.

In present paper, nanoindentation test and fretting wear experiments were conducted to investigate the adhesion, fretting behavior and wear mechanism of TiN, CrN and TiN/CrN superlattices with different superlattice period Λ, deposited on WC/Co cemented substrate by reactive magnetron sputtering. The morphology of wear scar was observed and analyzed by SEM, surface roughness profilometer. SEM element imaging was used to analyze the Fe element distribution on the wear scar.

2. EXPERIMENTS

2.1 Substrate

Ground and subsequently polished WC/Co (10×10×1mm) cemented substrates were used in this study. The substrates were cleaned with trichlorethylene, acetone and alcohol in an ultrasonic clearer for 30 minutes.

2.2 Deposition

TiN/CrN superlattices are deposited with a reactive magnetron cathodic sputtering (RMCS) system used in RF mode on WC/Co cemented substrate. The sputtering system can be pumped down to less than 4×10^{-5}Pa (3×10^{-7}Torr). Argon and Nitrogen gas of very high purity (99.999%) is introduced into chamber, a throttle valve controls the gas pressure. The distance between the substrate holder and the target (diameter 5 cm) is 2 cm. The target power was kept constant at 200W, while the N_2 was fed into the chamber through a separate gas manifold located in the vicinity of the target, the ratio of Argon to Nitrogen is 5:1 that produced stoichiometric TiN and CrN coatings. Prior to any deposition, the metal (Ti, Cr) target (purity 99.95) is cleaned by "presputtering" for about 20 minutes while the substrates are isolated from the plasma by a shutter. The ratio of single layer thickness is 1:1 and the superlattice

period is controlled from 5.4 to 55nm by keeping the substrates alternately stationary above the Ti and Cr target, and the total thickness was about 2, 4, 6 μm, respectively, to warrant having enough thickness to be worn. The substrate temperature during deposition was kept at 500 ± 10℃. Ti underlayer was 30Å for all samples and TiN was 100Å as buffer layer for all samples. The low-angle and middle-angle X-ray diffraction experiments were conducted to very the superlattice construction of TiN/CrN superlattices.

2.3 Fretting wear and assessment

The fretting wear experiment apparatus is that the normal contact load and the tangential force are applied to the upper specimen. The data of friction coefficient were measured and recorded by a personal computer through strain gauges, amplifier and A/D board.

The fretting experiments were conducted using the 'ball-on-disc' arrangement at the sliding amplitude about 80 μ m, frequency at 10Hz. The average sliding velocity is 0.8mm/sec. The applied normal load is 4N, and the fretting cycles are about 5×10^3,10^4, 5×10^4 respectively. The upper specimen was an SJU2-QT bearing steel ball with a diameter of 9 mm, and the below specimen is TiN, CrN single layer films and TiN/CrN superlattices with the area of 100 mm^2.

The profiles of fretting scar area, wear volumes were obtained by the surface roughness profilometer. Wear volume is divided into heap volume (V_H) above the datum line and scar volume (V_S) below the datum line, and using net wear volume loss ($V_N = V_H - V_S$), obtained from the scar volume subtract the heap volume, to assess the wear volume of coatings.

3. RESULTS

3.1 Structure of coatings

The structure and crystal orientation of TiN, CrN single layer films and TiN/CrN superlattices deposited on WC/Co cemented substrate was determined by X-ray diffraction (XRD). Figure 1 shows the middle angle x-ray diffraction patterns of Substrate, TiN, CrN and TiN/CrN superlattices with superlattice period Λ = 5.4 nm. Cubic CrN single layer film indicates a (200)-preferred orientation. For TiN single layer film, however, did not show (111) or (200) preferred orientation, just showed similar intensity at (111), (200) and (311) reflection peak and did not exhibit the strong (111) preferred orientation as deposited on HSS substrate or on other substrates. First order satellite peaks around the (111) and (200) Bragg reflection were observed for TiN/CrN superlattices with Λ = 5.4 nm. Especially, TiN/CrN superlattices deposited on WC/Co substrate shows a strong (200)-preferred orientation as shown in figure 1. With increasing of superlattice period Λ, the main peaks would shift to lower angle side. Low-angle XRD spectra from all superlattices showed the several superlattice reflection peak.

3.1. Hardness anomaly

Hardness and elastic modulus data were measured using an Elionix ENT-1100 nanoindentation tester, which continuously monitors the displacement of a triangular-pyramid diamond indenter tip as a function of the load on the tip, and the load on the tip was 5mN. Hardness value vs. superlattice period Λ is shown in

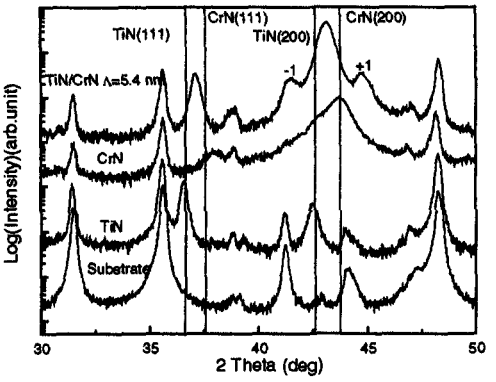

Figure 1 Middle angle X-ray diffraction patterns of TiN, CrN and TiN/CrN superlattices with Λ = 5.4 nm

Figure 2, and exhibits the hardness anomaly for TiN/CrN superlattices deposited on WC/Co cemented substrate, and the maximum enhancement of 50% occurs at the superlattice period Λ = 15~21 nm. The increase of hardness would contribute to the enhancement of the

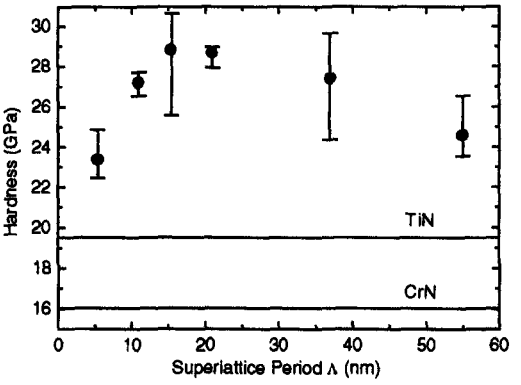

Figure 2 Hardness vs. superlattice period of TiN/CrN superlattices

resistance to plastic deformation of films, and would be expected to decrease the friction coefficient and wear volume of superlattices.

3.2 Coefficient of friction

Figure 3 shows the friction coefficient of TiN, CrN single layer films and TiN/CrN superlattices after 10^4 cycle numbers. The friction coefficient of TiN/CrN superlattices indicated a similar tendency with CrN single film that these values will decrease after 10^3 cycles and located from 0.15 to 0.25, and CrN and TiN is 0.12 and 0.30 respectively. The low friction coefficient of CrN single layer film and TiN/CrN superlattices may relate to the oxidation of Ti and Cr. From the initial stage to 10^3 cycles, the friction coefficient of superlattices is larger than that of TiN and CrN single layer film because of smaller surface roughness for superlattices. The smaller surface roughness of superlattices generates the larger contact area between the contacting surface, which induce the larger friction coefficient during the initial fretting wear stage. Figure 3 is also shown that, with decreasing of superlattice period Λ, the friction coefficient of superlattices was decreased. And opposites to this, with increasing of superlattice period, superlattics become easy to detach because of weak bonding strength

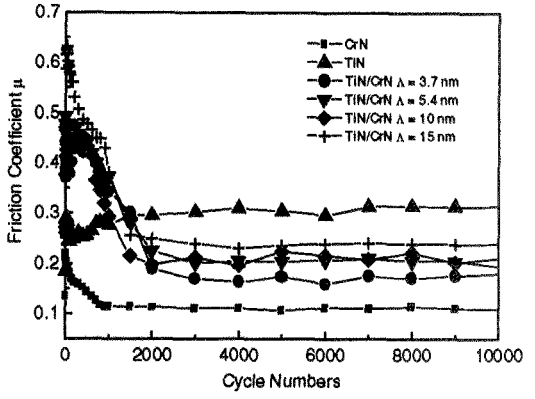

Figure 3 Friction coefficient vs. cycle numbers of TiN, CrN and TiN/CrN superlattices

between layers and would induce the increasing of friction coefficient.

3.3 Wear volumes

Figure 4 shows the comparison of the net wear volume between TiN single layer film and superlattices with Λ= 21nm, total film thickness are 2, 4, 6 μ m respectively. After 5×10^4 fretting cycle numbers, the net wear volume of superlattices is about one fifth of

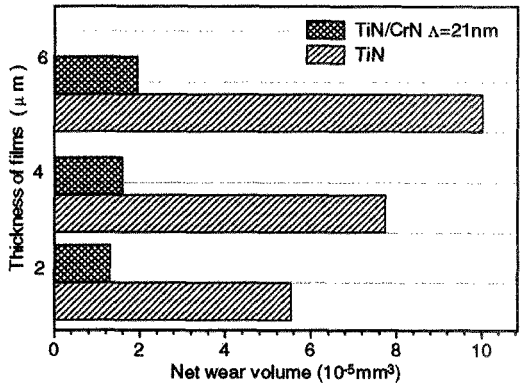

Figure 4 Comparison of net wear volume between TiN and TiN/CrN superlattices

that of TiN, it means that the wear-resistance of superlattices is improved remarkably with superlattice film technology. The improved wear-resistance for TiN/CrN superlattices are contributed from many factors including the enhancement of hardness and elastic modulus, higher resistance to plastic deformation, the formation of dense Cr_2O_3 and TiO_2 oxide layer on the wear scar surface, the improvement of adhesion and the decrease of friction coefficient.

4.WEAR SCAR PROFILES & MORPHOLOGY

Figure 5 shows the wear scar profiles of CrN, TiN and TiN/CrN superlattices with Λ = 21 nm after 5×10^4 fretting cycles. CrN single layer film shows a partial stick area on the surface of wear scar and a plastic domain in the side of stick area and the edge of wear scar of because of low hardness and low resistance to plastic deformation. TiN film, with 2 μm total thickness, exposes the substrate material as shown in figure 5 after 5×10^4 fretting cycles and the depth of wear scar reach

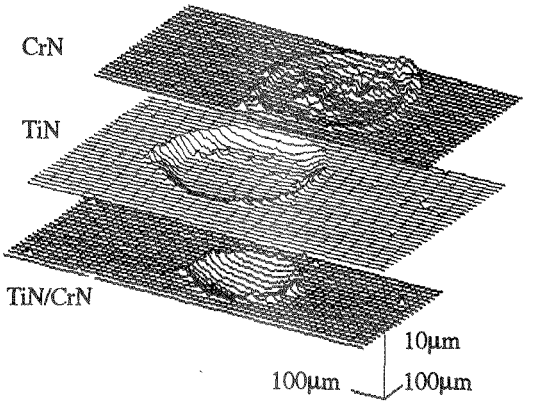

Figure 5 Typical wear scar profiles of CrN, TiN and TiN/CrN superlattices with Λ = 21 nm

to 2.6 μm for 4 μm total thickness film after 5×10^4 fretting cycles. TiN/CrN superlattices showed smaller fretting wear scae area than that of CrN and TiN single layer film and the depth of wear scar was just 0.6μm after 5×10^4 fretting cycles, which benefit from the low crack penetration rate for multilayers. For TiN/CrN superlattices, the stick contact radius c became smaller and even to zero due to the enhancement of hardness, elastic modulus and resistance to plastic deformation in comparison with TiN and CrN single layer films. It

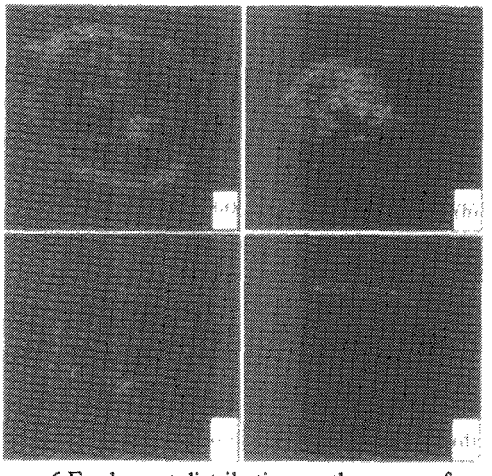

Figure 6 Fe element distribution on the scar surface of CrN(a), TiN(b), TiN/CrN superlattices with Λ = 5.4, 55 nm (c) and (d)

means that the wear mechanism of superlattices changed from mixed stick-slip to gross slip regime. Superlattices with Λ = 21 nm showed, that the depth of wear scar was just 0.6 μm after 5×10^4 cycles,

The adhesion behavior of TiN, CrN and TiN/CrN superlattice was also analyzed TiN by SEM imaging of Fe element as shown in figure 6. Figure 6 (a) shows that the stuck Fe element distributes in the center and at the edge of CrN film due to the high affinity with Cr and low hardness foe CrN film. TiN single layer film, has been known as the column growth and the higher surface roughness, exhibit half of the scar area was stuck with Fe from the bearing ball. Cracks were generated in these stuck third bodies under fretting load and tend to penetrate into the surface of TiN. Severe adhesion would

induce the higher tangential force Q_x under fretting load, which would cause the detaching from substrate for CrN film possessing weak bonding strength with WC/Co substrate, and the forming and the connection of microcracks in TiN single layer film. TiN/CrN superlattices shows, whereas, that almost no Fe cluster was observed on the surface of superlattices wear scar by SEM imaging technology as shown in figure 6 (c) and (d) from $\Lambda = 21$ to 55 nm.

The morphology of surface before and after fretting wear was also observed by SEM as shown in figure 7 (a) ~ (d). Figure 7 (a) shows the detaching of CrN single layer film from WC/Co substrate after 5×104 fretting cycles. TiN single layer film possesses a higher surface roughness after deposition as shown in figure 7 (b), the rms (Rq) was 16.52 nm and the maximum height (Rmax) was 107.62 nm, measured with AFM. The higher surface roughness would induce the severe adhesion wear as shown in figure 6 (b). Figure 7 (c) shows the flat fretting wear surface for TiN/CrN superlattices with Λ = 21 nm. With increasing of superlattice period, as shown in figure 7 (d) with Λ = 55 nm, superlattices tend to delaminate because of weak bonding strength between layers and extend to generate

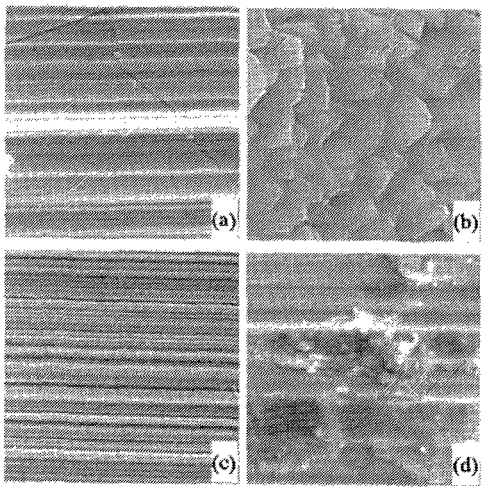

Figure 7 SEM mophology of CrN (a), TiN (b), TiN/CrN superlattices with Λ = 21 (c) and 55 nm (d) respectively

crack in these larger debris. The larger debris would induce the increasing of friction coefficient and wear volume.

5. SUMMARY

1. TiN/CrN superlatives showed the anomaly of hardness at $\Lambda = 15 \sim 21$ nm with an increase of 50% and gained the higher ductility simultaneously in comparison with TiN. The friction coefficient of TiN/CrN superlatives located between 0.15 to 0.25, CrN and TiN is 0.12 and 0.30 respectively. The net wear volume of superlatives was just about one fifth of that of TiN single layer film after 5×10^4 fretting cycles.
2. The adhesion of TiN/CrN superlatives was improved due to the enhancements of hardness, elastic modulus and the resistance to plastic deformation. The wear mechanism was transferred from mixed stick-slip to gross slip regime for TiN/CrN superlatives.
3. TiN/CrN superlatives overcame the shortcoming for CrN single layer film deposited at 500℃, the weak bonding strength with WC/Co substrate and the generation of detaching during fretting wear. TiN/CrN superlattice technology improved the film surface roughness also.
4. The optimum superlattice period Λ, for eliminating the adhesion and gaining excellent fretting properties, was $\Lambda = 15 \sim 21$ nm for present TiN/CrN superlattices, that exhibited the hardness anomaly.

6. ACKNOWLEDGE

The authors would like to thank Mr. N. Shim and Mr. H. Ueda (Hitachi tool Ltd.) for their kind help in nanoindentation measurements and applying of WC/Co cemented substrate, and also gratefully thank Dr. T. Yamamoto and Dr. M. Fushitani for their appreciable discussion.

7. REFERENCE

[1] H. Randhawa, J. Vac. Sci. Technol. **A 4 (6)**, 2755-2758 (1986)
[2] S. Novak and M. Komac Wear **205**, 160-168 (1997)
[3] Z.P. Huang, Y. Sun and T. Bell, Wear **173**, 13-20 (1994)
[4] T. Sato, Y. Tada, M. Ozaki, K. Hoke and T. Besshi, Wear **178**, 95-100 (1994)
[5] J.F. Lin, M.H. Liu, and J.D. Wu, Wear **199**, 1-11 (1996)
[6] Y.L. Su, S.H. Yao and C.T. Wu, Wear **199**, 132-141 (1996)
[7] E.J. Bienk and N.j. Mikkelsen, Wear **207**, 6-9 (1997)
[8] S. Hogmark and P. Hedenqvist, Wear **179**, 147-154 (1994)
[9] W.-H. Soe, R. Yamamoto, Materials chemistry and physics **50**, 176-181 (1997)
[10] P. Yashar, S.A. Barnett, J. Rechner and W.D. Sproul, J. Vac. Sci. Technol. **A 16 (5)**, 2913-2918 (1998).
[11] J.S. Koehler, Phys. Rev. **B2,** 547 (1970).
[12] E.O. Hall, Proc. Phys. Soc., Ser. **B 64,** 747 (1951).
[13] N.J. Petch, J. Iron Steel Inst., **41,** 25 (1953).
[14] C.Subramanian and K. N. Strafford, J. Mater. Sci. **31,** 5907-5914 (1996).
[15] R.J. Zhang, Z.W. Lin, Zh.P. Cui and Q. Song, Wear **147,** 227-251 (1991).
[16] W. Zhang and Q.J. Xue, Wear **214,** 23-29 (1998).
[17] S.R. Brown, Materials Evaluation under fretting conditions, ASTM Spec. Tech. Publ. 780, Warminster, PA, 1981.

(Received December 11, 1998; accepted February 28, 1999)